

U. Ganzer
 Technische Universität Berlin, Germany

Abstract

2D model tests have been made in a test section with flexible top and bottom wall. A conventional NACA 0012 aerofoil and a supercritical CAST 7 aerofoil have been used both with a tunnel height to chord ratio of 1.5. It is shown that wall interference effects can be reduced substantially by wall shaping and that transonic blockage can be avoided.

The same test section was used for 3-component force-measurement on a simple swept-wing-body-combination in order to demonstrate convergence of the adaption process for 3D model tests.

Future work will entail 3D measurements in a test section with eight flexible walls. The design of the test section is outlined. It has an octangular cross-section. Each of the eight walls will undergo only two-dimensional deformation in an identical way to those in the 2D experiments.

1. Introduction

In general the walls of a wind tunnel test section effect the flow around the model. The measured aerodynamic data have to be corrected for wall interference effects. In addition, at transonic speeds, solid walls lead to blockage effects: When sonic speed is reached in the cross-section of minimum open area the mass flow is at its maximum. The tunnel flow is choked and it is not possible to increase the main stream Mach number furthermore. Ventilated walls - perforated or with longitudinal slots - avoid such blockage. However, wall interference corrections become more difficult, because of the complicated boundary condition at the wall.

Adaptive flexible wind tunnel walls, in principle, can avoid transonic blockage and reduce wall interference effects to be negligible. It requires a wall-shaping appropriate to the streamline curvature of an unrestricted flow around the model.

2. The principle of wall adaption

An adapted wind tunnel wall can be considered as a substitute for a stream surface in an unrestricted flow field, Figure 1.

The remarkable property of a stream surface is that it cannot sustain forces. Therefore the pressure on both sides of the surface must be the same; there might be a pressure gradient but no

pressure jump. This condition can be used to check whether the wall shape corresponds to that of a stream surface. One can measure the pressure distribution along the wall inside the tunnel. This is the real part of the unrestricted flow field. Along the outer side of the wall the flow does not exist, it is just fictitious. But one can calculate the pressure for the fictitious flow over the known wall shape taking the same main stream condition as it exists for the tunnel flow. Only if both pressure distributions - the calculated and the measured one - are the same, the wall shape can be considered as adapted.

If there is a difference in the pressure distributions, this difference can be used for an iterative adaption procedure. Something like a mean value between the two pressures can be taken to calculate a new wall shape which would in the fictitious flow produce this mean pressure distribution. (More precisely a relaxation factor is used so that not an exact mean value is taken but more weight is given to the calculated (external) pressure distribution. The external pressure distribution is found to be less sensitive to changes in wall contour.) The wall is then deformed according to the calculated new shape and again the pressure distribution is measured and compared with the one just prescribed for the fictitious outside flow field. The procedure will be repeated until the differences are within a prescribed margin.

This principle of wall adaption has been applied successfully not only to flexible wind tunnel walls (1,2,3,4) but also - in an equivalent manner - to porous walls with variable suction (5,6,7).

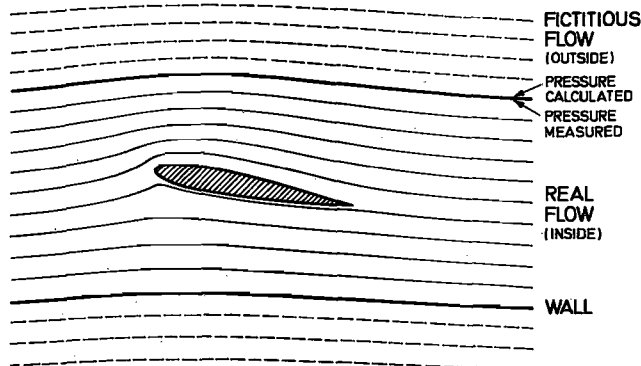


FIGURE 1. The principle of adaptive walls

⁺⁾ This research is supported by the German Ministry of Science and Technology (BMFT) and the German Research Ass. (DFG)

3. The 2D Case

3.1 Test section design and wall control

A sketch of the 2D test-section with adaptive flexible walls is shown below, Figure 2. This is an improved design based on the experience gained from earlier investigations (3,8).

The two flexible walls are made of glas fiber. Eight jacks are attached to each wall allowing wall displacement up to ± 25 mm. The jacks are driven by electro-motors. The displacement can be measured by potentiometers with an accuracy of $7/100$ mm. The entire wall adaption procedure is arranged with fully automatic control by a HP 1000F Computer. The computer controls the scarnivalves and stores the pressure distribution measured along the wall (as well as all test data for the aerofoil). On the other hand the wall shape is measured by the potentiometer readings. The first iteration in the adaption process requires a pressure distribution to be calculated which the measured wall-contour would produce in the fictitious exterior flow. The next step is then to use an intermediate pressure distribution between the calculated and the measured one for calculating a wall contour which would produce this pressure distribution in the fictitious exterior flow. In both cases subsonic small perturbation theory is being used. Typical computer time for the calculation in the course of one iteration is 8 seconds. The test-section walls are then set according to the calculated shape. The computer controls the wall deformation in such a way that all electro-motors start moving at the same time, but their speed is different. The jack which has to produce the largest displacement is driven with maximum speed. The movement of the other jacks is differentiated accordingly, so that they all reach their final position at the same time. The method of operation is summarised in the flow diagram of Figure 3. More details are given in (9).

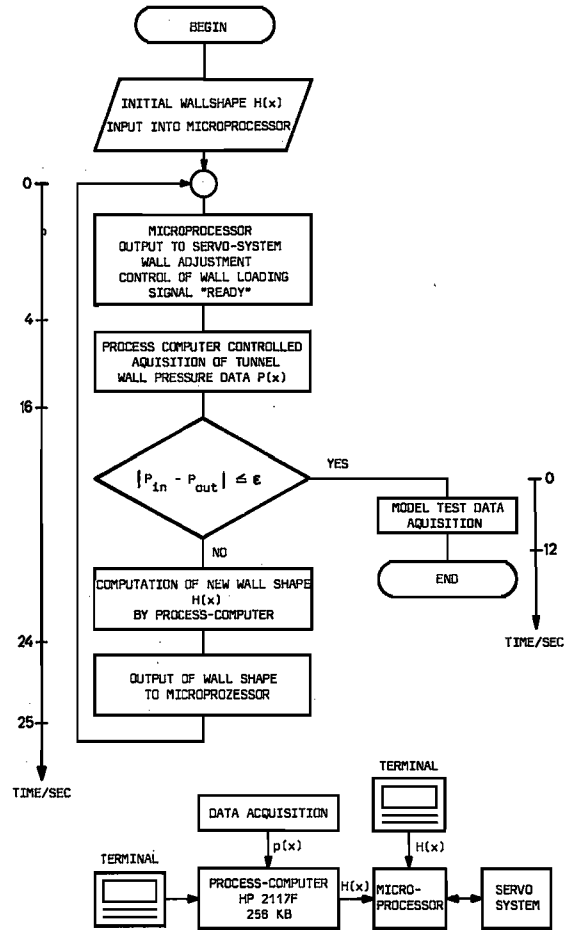


FIGURE 3. Flow diagram of wall control and tunnel operation

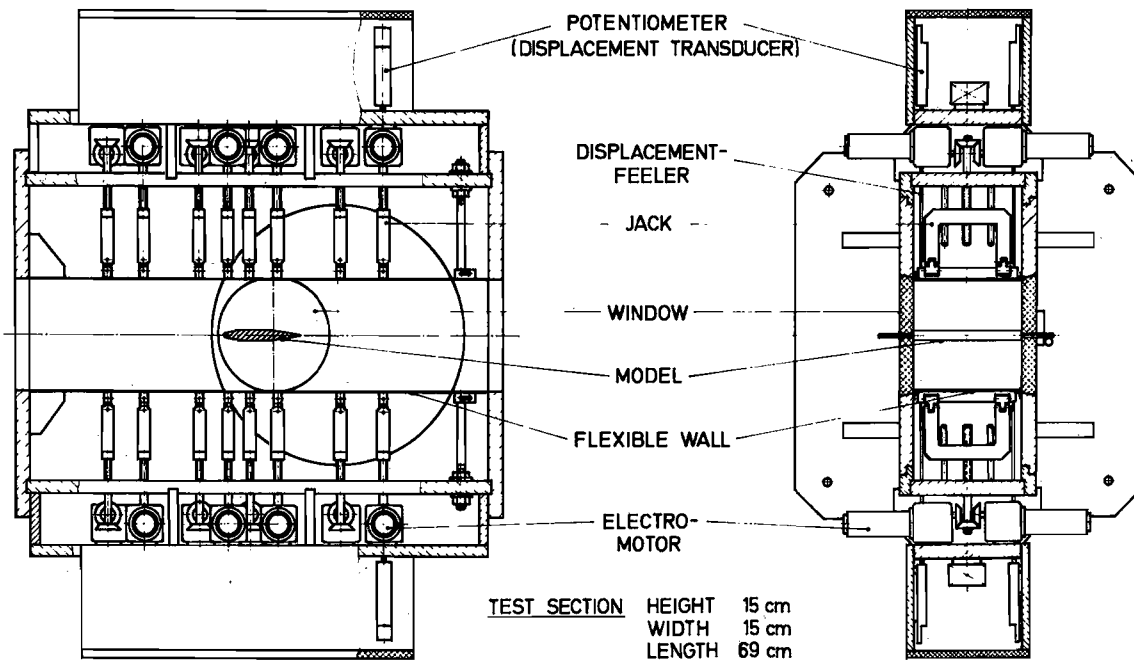


FIGURE 2. The 2D test section with adaptive walls

3.2 Test results for NACA 0012 aerofoil

The NACA 0012 aerofoil had been chosen as a test model because of the large amount of data available for it from tests in other wind tunnels. The first results obtained in the TU Berlin tunnel with adaptive walls were presented in (3). They had suffered from a lack of model accuracy and from the small number of pressure taps. Therefore some of the test cases have been repeated using another model of higher accuracy and with a fairly large number of pressure taps. The aerofoil chord was kept to 10 cm providing tunnel height to chord ratio of 1.5.

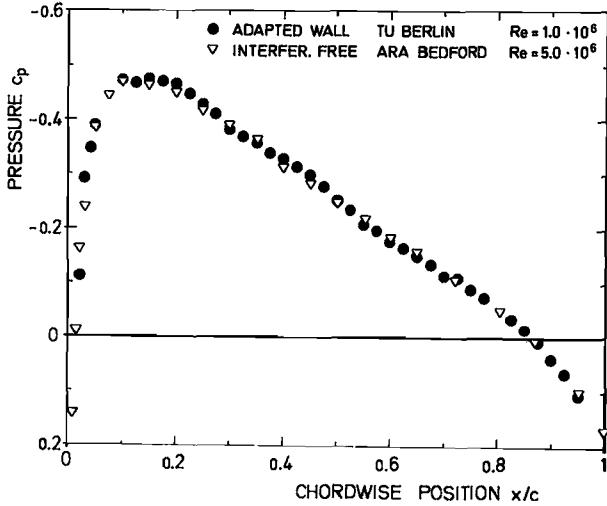


FIGURE 4. Pressure distribution for NACA 0012
Free transition $M_{\infty} = 0.50$ $\alpha = 0^\circ$

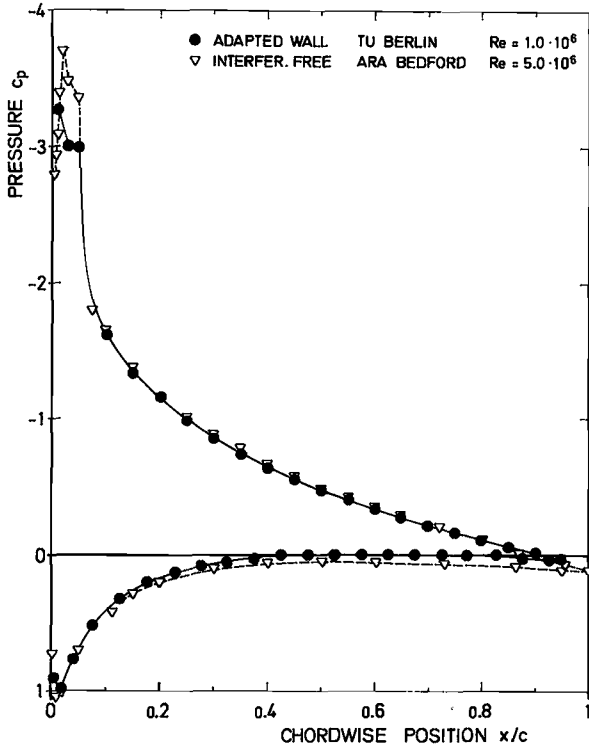


FIGURE 5. Pressure distribution for NACA 0012
Free transition $M_{\infty} = 0.50$ $\alpha = 7.686^\circ$

Test results for subcritical flow condition compare well with ARA Bedford data, Figure 4. The ARA data were taken in 8"x18" tunnel with a tunnel height to model chord ratio of 3.6. The top and bottom wall of that tunnel is slotted. The data had been corrected for interference effects (11).

A series of tests was made at $M_{\infty} = 0.5$ for a range of angle of attack (10). The main purpose of these tests was to clarify whether wall adaption was possible with flow separation at the aerofoil. As a result it can be stated that adaption was achieved even for angles of attack much beyond stall. In Figure 5 the pressure distribution is shown just before stall. Oilflow pictures did confirm the existence of a small separation bubble near the leading edge and diminishing skin friction on the rear part of the aerofoils upper surface. Differences in the pressure distributions measured at ARA Bedford and TU Berlin are at least partly attributed to the differences in Reynolds number.

One way of judging the convergence of the wall adaption process is by observing the variation of wall displacement. From one iteration step to the other the required change in wall displacement is expected to decrease and finally reach some prescribed limit. Usually a limit is set to the wall adjustment by the accuracy of the jacks and/or the potentiometer readings. The

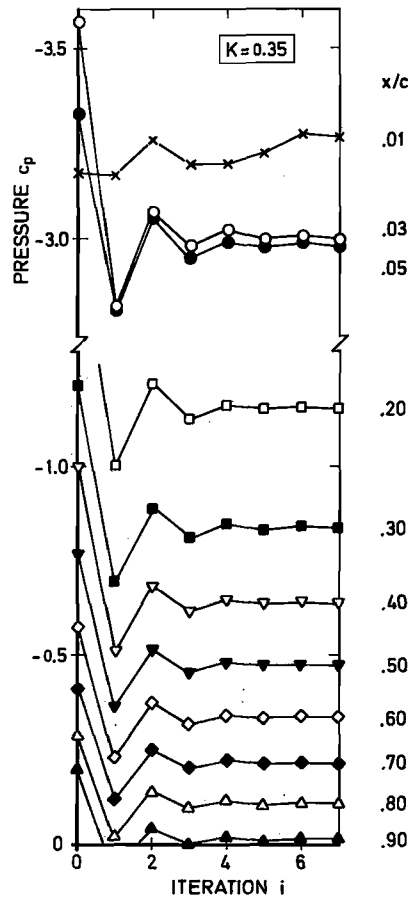


FIGURE 6. Local pressure variation on NACA 0012
Upper surface $M_{\infty} = 0.50$ $\alpha = 7.686^\circ$

question arises whether the accuracy of the wall setting can in all cases be taken as a direct measure of the accuracy of the test data. In particular when the flow over an aerofoil gets separated, it might be expected that even very small changes in wall contour could have a pronounced impact on the aerofoil flow.

In order to judge the sensitivity of the local aerofoil flow pattern to the changes in tunnel wall shape the pressure measured has been plotted for each pressure tap as it varies during the iterative adaption procedure, Figure 6. The adaption did start from the plane wall configuration (Iteration 0). In the particular case shown the pressure readings indicate some scatter for the 1% chord station very near to the leading edge. This is for the pressure tap just at the separation line of the small local separation bubble. The scatter reflects the slightly unsteady nature of the separation. Similar results for other test cases including those with fully separated flow allow the conclusion that for subcritical flow conditions there is no particular sensitivity of the flow around the aerofoil to the changes in tunnel wall contour. The convergence of changes in wall displacement or wall pressure distribution could be taken as a direct measure of the convergence of the aerofoil pressure distribution.

For practical operation of a wind tunnel with adaptive walls however there is the need for a fast and reliable measure of convergence and at the same time some information is required about the residual scatter of the test data. It was felt that the mean value of the pressure measured at the various taps on the upper surface of the aerofoil will be the best and most adequate measure. In Figure 7 this value is plotted for the case with flow conditions just before stall.

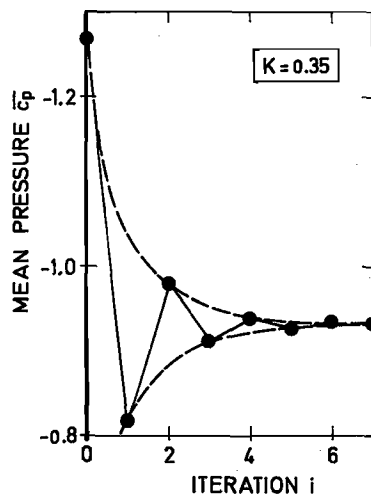


FIGURE 7. Variation of mean pressure
NACA 0012 $M_{\infty} = 0.50$ $\alpha = 7.686^{\circ}$

In Figure 8 a similar plot is shown for a slightly higher angle of attack representative for flow conditions beyond stall. The three curves show different convergence. This is due to a different relaxation factor used in the adaption procedure. While for small angles of attack a factor of $K = 0.35$ was found to be optimal here a relax-

ation factor of $K = 0.25$ was leading to fastest convergence. Only two iterations were needed to arrive at the adapted wall shape.

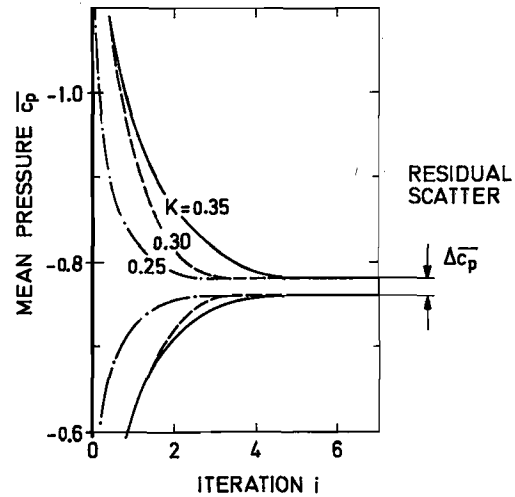


FIGURE 8. Variation of mean pressure
NACA 0012 $M_{\infty} = 0.50$ $\alpha = 7.686$

The high angle of attack case with extensive flow separation at the aerofoil exhibits fairly large residual scatter of the mean pressure coefficient. This reflects the unsteady nature of the flow. Before stall however the residual scatter is very small, Figure 9.

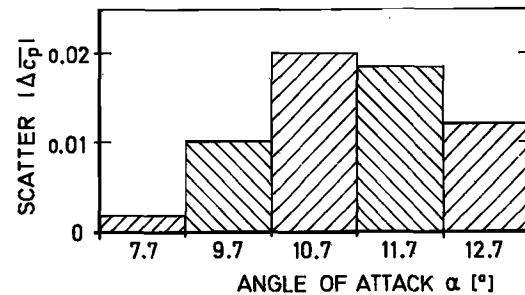


FIGURE 9. Residual scatter of mean pressure
NACA 0012 $M_{\infty} = 0.50$

Only two further tests have been performed with NACA 0012 at supercritical flow conditions.

At $M_{\infty} = 0.55$ and $\alpha = 6^{\circ}$ a small supersonic region occurs near the leading edge of the aerofoil, Figure 10. Comparison with interference-free test data from Calspan (5) at roughly the same Reynolds number show discrepancies which might be due to residual interferences as well as to differences in model geometry and/or roughness strip.

At $M_{\infty} = 0.80$ and $\alpha = 0^{\circ}$ a large supersonic region exists, Figure 11. Comparison with interference-free data from ONERA (12) indicates the importance of Reynolds number similarity for transonic testing. On the other hand great attention has to be given to the treatment of the transition strip.

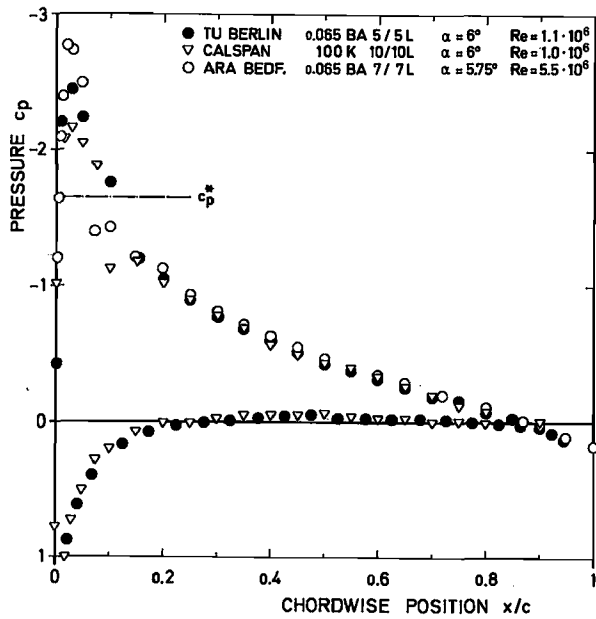


FIGURE 10. Pressure distribution NACA 0012
 $M_{\infty} = 0.55$ $\alpha = 6^{\circ}$

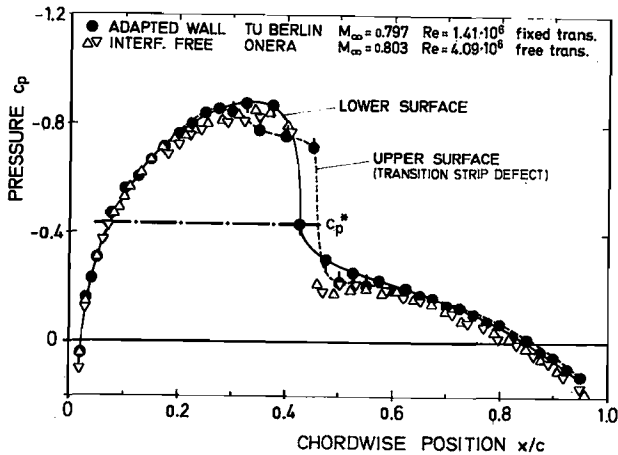


FIGURE 11. Pressure distribution NACA 0012
 $M_{\infty} = 0.80$ $\alpha = 0^{\circ}$

3.3 Test results for CAST 7 aerofoil

As the testing of supercritical aerofoils will be the main concern of 2D transonic wind tunnels it seems to be of great interest to demonstrate the capabilities and the limits of a test section with adaptive walls by using a supercritical aerofoil. A test programme that is considered to be representative for practical transonic aerofoil testing is shown in the table, Figure 12.

The CAST 7 aerofoil had been chosen as a test model because it is thought to be representative of the current state-of-the-art supercritical aerofoils and it also has fairly widely been tested in other wind tunnels. As compared with the NACA 0012 aerofoil it will produce a fairly large supersonic region with only small terminating shock.

| α \ M_{∞} | .60 | .65 | .70 | .72 | .74 | .75 | .76 | .77 | .78 | .79 | .80 | .82 |
|-------------------------|-----|-----|-----|-----|-----|-----|-----|-----|-----|-----|-----|-----|
| -2.0 | ○ | | ○ | | | | | ○ | | | | |
| -1.0 | ○ | | ○ | | | | | ○ | | | | |
| 0 | ○ | | ○ | | | | | ○ | | | | |
| * | ○ | ○ | ○ | ○ | ○ | ○ | ○ | ○ | ○ | ○ | ○ | ○ |
| 1.0 | ○ | ○ | ○ | ○ | ○ | ○ | ○ | ○ | ○ | ○ | ○ | ○ |
| ** | ○ | ○ | ○ | ○ | ○ | ○ | ○ | ○ | ○ | ○ | ○ | ○ |
| 1.5 | | | | | | | ○ | | | | | |
| 2.0 | ○ | | ○ | | | | | | | | | |
| 2.5 | | | | | | | ○ | | | | | |
| 3.0 | ○ | | ○ | | | | | | | | | |
| 3.5 | | | | | | | ○ | | | | | |
| 4.0 | ○ | | ○ | | | | | | | | | |
| 4.5 | | | | | | | ○ | | | | | |
| 5.0 | ○ | | ○ | | | | | | | | | |
| 5.5 | ○ | | ○ | | | | | | | | | |
| 6.0 | ○ | | | | | | | | | | | |
| 6.5 | ○ | | | | | | | | | | | |
| 7.0 | ○ | | | | | | | | | | | |
| 7.5 | ○ | | | | | | | | | | | |
| 8.0 | ○ | | | | | | | | | | | |

* providing $C_A = .5$ at $M_{\infty} = .76$
 ** providing $C_A = .6$ at $M_{\infty} = .76$

FIGURE 12. Test program CAST 7 aerofoil

That is to say that the supersonic region might well extend to the wind tunnel upper wall but the shock will not reach the wall. Thus, for quite a few test cases shock boundary layer interaction on the wind tunnel wall will not dominate the flow field but an interaction of the nearly shockless supersonic region with the wall and its boundary layer. It remains to be seen whether this will create particular problems to the use of adaptive walls in wind tunnel testing.

The first tests with CAST 7 aerofoil reveal the sensitivity of a supercritical aerofoil to Reynolds number and transition fixing. Our test data had been obtained at Reynolds number slightly above 1 Million while for direct comparison DFVLR

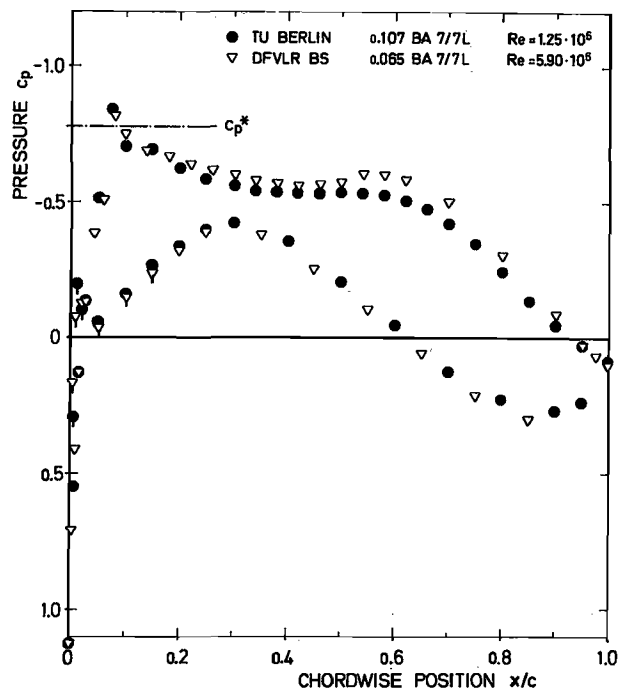


FIGURE 13. Pressure distribution CAST 7
 $M_{\infty} = 0.70$ $\alpha = 0^{\circ}$

data were available at Reynolds number 6 Million [12]. In addition only a few unpublished data had been used from DFVLR at 1.5 Million Reynolds number.

Already at subcritical flow conditions discrepancies occur between the test results for different Reynolds numbers, Figure 13. Results were also available for $Re = 1.48 \cdot 10^6$ and $\alpha = -0.04^\circ$. These are not shown as they are identical with our results (full points) except for very small discrepancies close to the leading edge and at the trailing edge.

At higher Mach number the differences in the pressure readings around the 60 % chord position become more pronounced for the two tests at different Reynolds number, Figure 14a. These differences are eliminated when Reynolds number is roughly the same, Figure 14b. For the comparison of pressure distributions near the nose it has to be no-

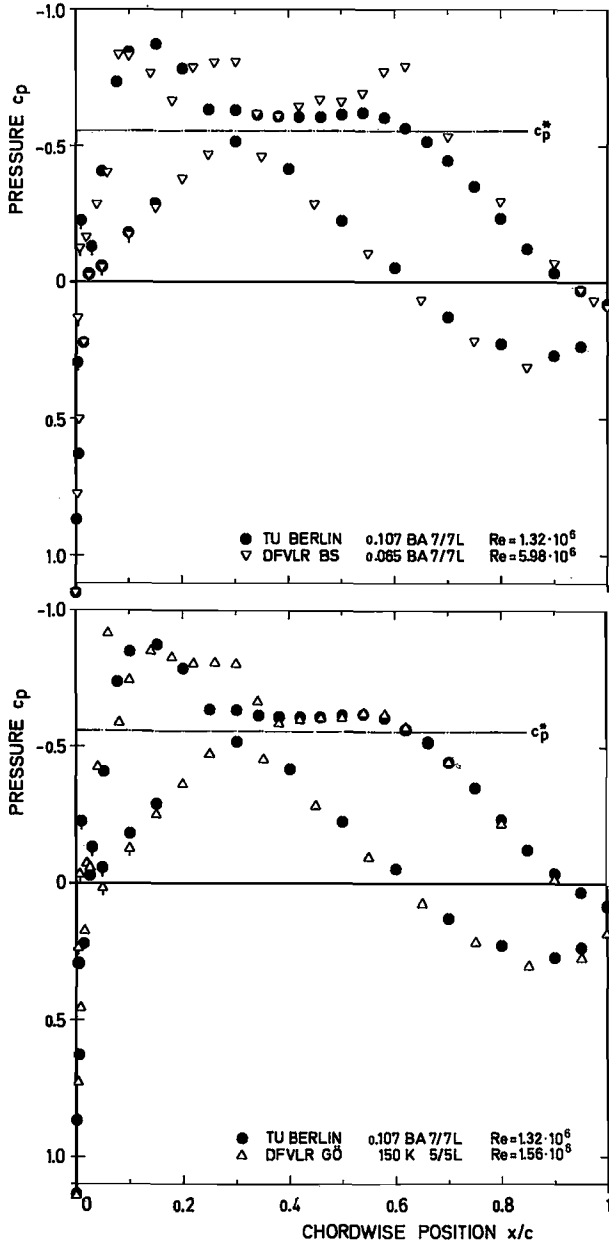


FIGURE 14a and 14b. Pressure distribution CAST 7
 $M_{\infty} = 0.76$ $\alpha = 0^\circ$

ted that on our model the transition strip was interrupted to keep the 7.5 % pressure tap free. But as the pressure taps were located along a curved line across the chord, the 10 % tap was already behind the full transition strip.

At higher angle of attack the differences in the pressure curves, Figure 15 and Figure 16,

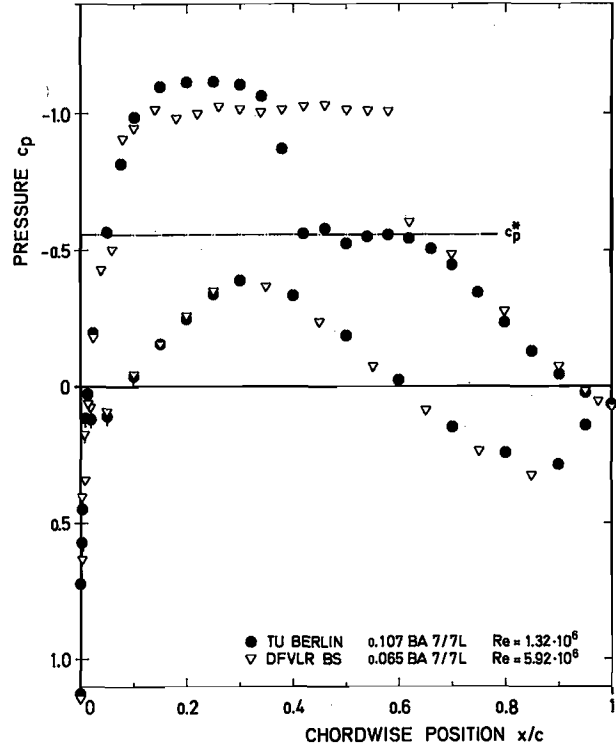


FIGURE 15. Pressure distribution CAST 7
 $M_{\infty} = 0.76$ $\alpha = 1^\circ$

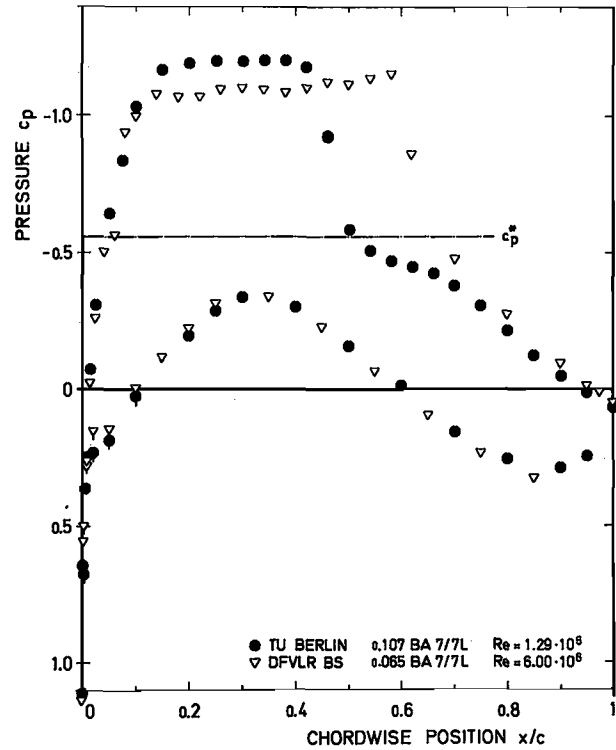


FIGURE 16. Pressure distribution CAST 7
 $M_{\infty} = 0.76$ $\alpha = 1.5^\circ$

might again - at least partly - be attributed to the different Reynolds numbers. DFVLR data for lower Reynolds number are available only for different angle of attack. Interpolation between these data show that for the lower Reynolds number the shock position would be further upstream and the negative pressure level in the supersonic region would be increased. However the interpolated data do not quite coincide with our results.

All the argumentation above is based on the assumption that wall interference is negligible in our test section with adapted walls. Whether this assumption really holds can finally be proved only by testing the same model with the same transition strip at the same Reynolds number in a larger wind tunnel. Such tests are planned in the DFVLR 1 x 1 m transonic facility for end of 1980.

4. The 3D case

4.1 A 3D model in the 2D tunnel

As a provisional test of a 3D model in a wind tunnel with adaptive walls a simple wing-body combination has been tested in the 2D test section. The model was available from earlier calibration tests (13). It has a swept wing of aspect ratio $\Lambda = 2.75$. The body is cylindrical with an ogive nose.

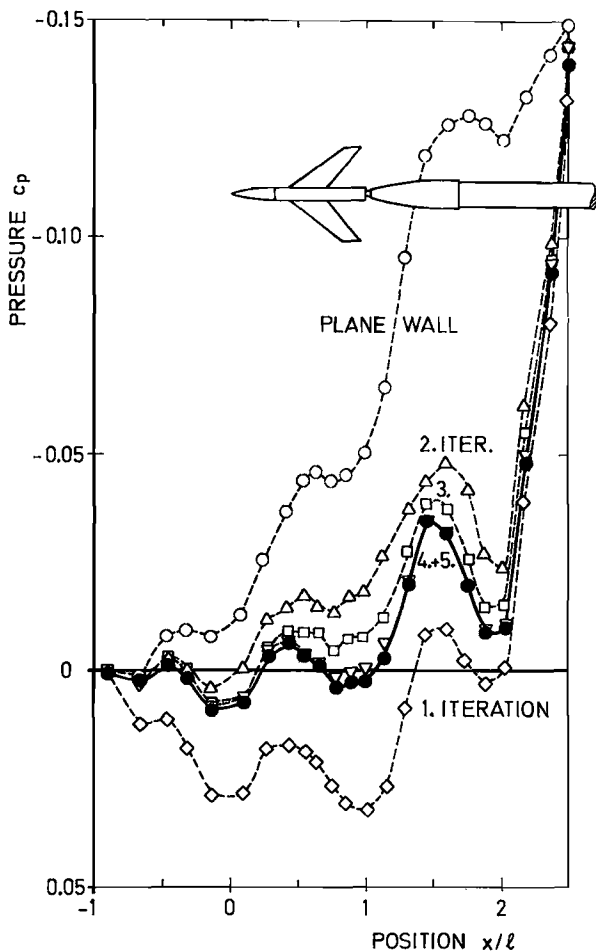


FIGURE 17. Pressure along center line of the flexible wall
Model F1 $M_{\infty} = 0.80$ $\alpha = 0^\circ$

A six-component balance was used for a few force measurements. The main drawback of the experimental set-up was that the drag balance was an external balance giving higher blockage to the flow than the model.

The main purpose of the test was to show, that wall adaption is possible even when the model blockage is comparatively small. (Blockage is described by the ratio between maximum cross-section area of the model and the cross-section area of the tunnel.) For the 2D tests the blockage was 8 % while for the wing-body-combination it is just 1.1 %. Therefore small pressure variation is expected along the tunnel wall leading possibly to insignificant changes of the wall contour. Problems would occur when these changes are just within the tolerances of the jacks and the displacement transducers. On the other hand if adjustment of the walls can be achieved a test section with two flexible walls could provide a solution to the problem to transonic blockage. Wall interference would still be high but amenable to theoretical correction methods for the boundary conditions are then much easier as with ventilated walls.

As an example wall pressure distributions and variations of wall shape are presented for a moderate Mach-number of $M_{\infty} = 0.6$ and zero angle of attack. It is shown that wall adjustment can be achieved although the pressure variation due to the model is indeed very small, Figure 17 and Figure 18.

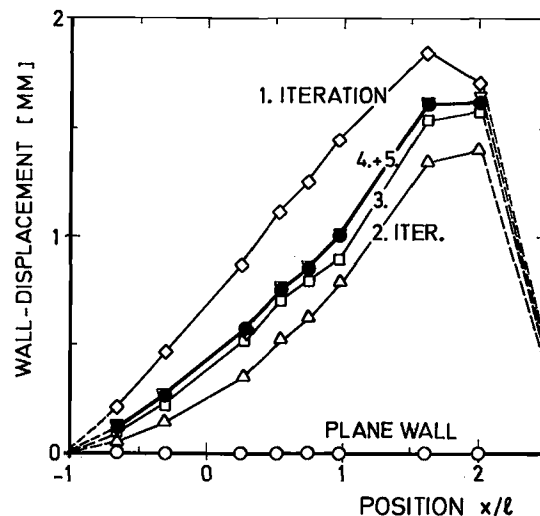


FIGURE 18. Displacement of the flexible walls
Model F1 $M_{\infty} = 0.80$ $\alpha = 0^\circ$

4.2 The 3D test-section design

A sketch of the 3D test-section design with eight adaptive walls is shown below, Figure 19. The eight walls will undergo twodimensional deformation in an identical way to that arranged in the 2D test section. Thus it is obvious that no complete 3D wall shaping is intended. However, it is believed that this compromise with regard to a limited number of variables and mechanical complexity will offer a practical solution.

In principle there are two main problems for the design and manufacture of the test section: The sealing at the corners between the individual walls and the installation of the model support. In addition problems occur from the small size of the test section: The space for the electro-motors and the potentiometers is fairly restricted and very high accuracy is required in particular for the jacks. Furthermore it is obvious that an internal drag balance should be available for the tests. This balance must have a diameter not more than 8 mm. Wing-body-combination testing will have to be restricted to force measurements. Surface pressure measurements will be possible with a body alone.

The sketch of the test-section design indicates that solutions have been found for the main problems. Spring steel lamellas can provide an adequate sealing of the octagon corners. In a mock-up it has been demonstrated that the surface can be kept very smooth. First wind tunnel tests with only one corner of the octagon tube show that the ventilation through the lamellas can be expected to be negligible.

The model support provides an angle of attack range of $\alpha = -3^\circ$ to $+13^\circ$. It is arranged to slide through the flexible walls. For reasons of flow symmetry as well as structural stiffness it was decided for a symmetrical support. The problem of allowing wall adjustment in the neighbourhood of the support was solved by a lateral displacement of the jacks, with a slightly different jack design.

The test section is expected to be ready for first tests at the begin of 1981.

4.3 The 3D test-cases

The main model to be tested in the octagon test-section will be a wing-body combination known as ZKP-F4. It is an Airbus-like configuration with

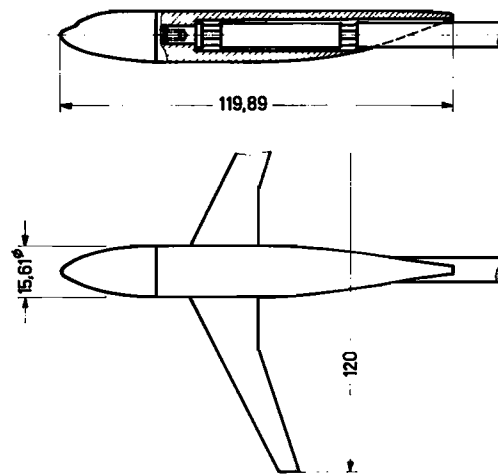


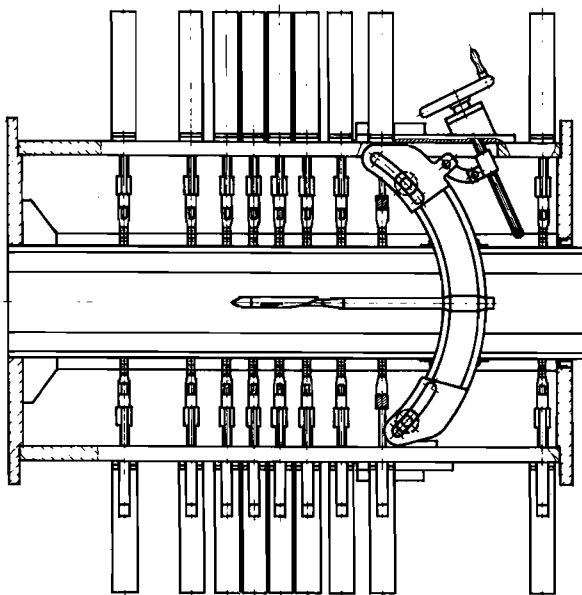
FIGURE 20. ZKP F4 model, Sting mounting

supercritical wing sections and wing aspect-ratio of $\Lambda = 9.5$, Figure 20.

As the span of the model is only 12 cm the relative accuracy is fairly poor. Interference free data will have to be obtained by testing the same model in a large wind tunnel. Therefore tests are being made with this model in the DFVLR 1 x 1 m transonic facility.

As a second model ONERA C 5 body of revolution will be tested, Figure 21. With this model pressure distributions can be obtained for a Mach number range up to low supersonic speed. Interference free data are available from (12).

It is hoped that with these two models it will be possible to demonstrate that in principle the octagon test section with adaptive wall can



TEST SECTION
 HEIGHT 15 cm
 WIDTH 18 cm
 LENGTH 85 cm

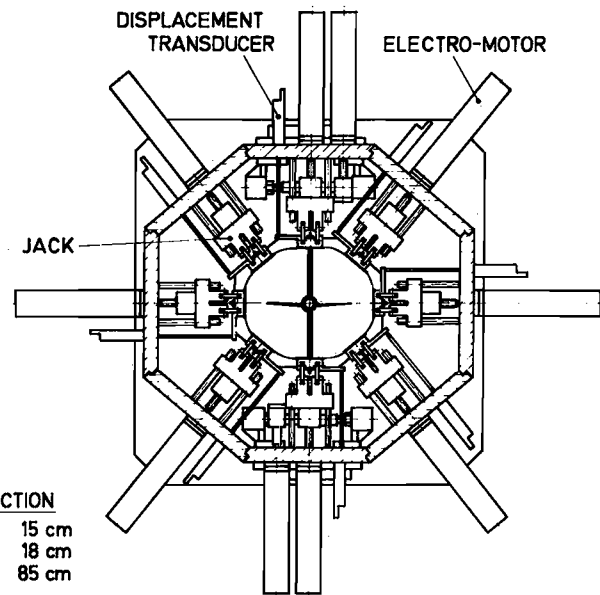


FIGURE 19. Design of the 3D test section with adaptive walls

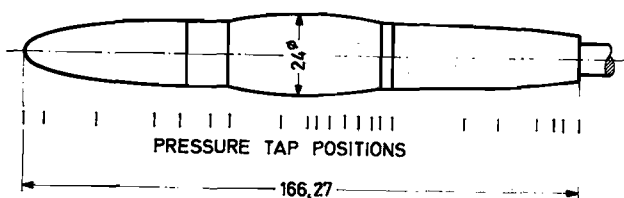


FIGURE 21. ONERA calibration model C5

avoid transonic blockage and reduce wall interference.

5. Conclusions

Test results for the conventional NACA 0012 and the supercritical CAST 7 show that substantial reduction in wall interference can be achieved and transonic blockage can be avoided in a test section with adapted walls. In addition tests with a 3D model in the tunnel with two adaptive walls give hope that the principle of wall adaption will generally be applicable to 3D model testing.

In order to get a comprehensive idea of the capability and limitations of the adaptable wall concept complete test series have to be carried out for a representative range of Mach number and angle of attack. The same models have to be tested in a large wind tunnel in order to obtain reliable interference free results for comparison.

Theoretical methods will have to be developed for residual wall interference corrections. At least for the 3D model tests such residual interferences are expected to be necessary. These interference corrections should be based on the measured wall pressure distributions.

At present calculation of the fictitious external flow field uses subsonic small perturbation theory. On the other hand no account is made for the boundary layer along the test section wall. The need for a fast calculation procedure makes it desirable to stick to that method, but it might become necessary to take into account transonic effects for the external flow field calculation and boundary layer development along the wall in the test section.

References

- (1) J.-P. Chevallier: "Parois auto-correctrices pour soufflerie transsonique." 12ème Colloque d'aérodynamique appliquée ENSMA / CEAT-Poitier, Nov. 1975
- (2) M.J. Goodyer: "The selfstreamlining wind tunnel" NASA TMX 72 699, Aug. 1975
- (3) U. Ganzer: "Windkanäle mit adaptiven Wänden zur Beseitigung von Wandinterferenzen." Z. Flugwiss. Weltraumforsch. Bd. 3, Heft 2, März-April 1979.
Translation: "Wind tunnels with adapted walls for reducing wall interference" NASA TM 75501, Aug. 1979
- (4) M.J. Goodyer and S.W.D. Wolf: "The development of a self-streamlining flexible walled transonic test section." AIAA Paper No. 80-0440, March 1980

- (5) R.J. Vidal, J.C. Erickson and P.A. Catlin: "Experiments with a self-correcting wind tunnel." AGARD CP 174, Oct. 1975
- (6) W.R. Sears et al.: "Interference-free wind-tunnel flows by adaptive-wall technology" Journ. of Aircraft, Vol. 14, No. 11, Nov. 1977
- (7) S. Bodapati, E. Schairer and S. Davis: "Adaptive-Wall Wind tunnel development for transonic testing." AIAA Paper No. 80-0441, March 1980
- (8) Y. Igeta: "Konstruktion und Erprobung von flexiblen Wänden für die Meßstrecke des ILR-Hochgeschwindigkeits-Windkanals." ILR TU-Berlin, Studienarbeit, Sept. 1978
- (9) J. Berg: "Entwicklung einer Prozeßrechner-gesteuerten Regeleinrichtung für die Adaption flexibler Windkanal-Wände." ILR Mitt. 70, TU Berlin, Juli 1980
- (10) J. Ziemann: "Das Konvergenzverhalten der Regelung adaptiver Windkanalwände bei Profiluntersuchungen im Hochstellwinkel-Bereich." ILR-Mitt. 66, TU Berlin, Jan. 1980
- (11) J. Sawyer: "Results of tests on aerofoil M.102/9 (NACA 0012) in the ARA 2D tunnel." ARA Model Test Note M.10219, Oct. 1978
- (12) J. Barche (Ed.): "Experimental Data Base for Computer Program Assessment." AGARD-AR-138, May 1979
- (13) U. Ganzer: "Eichversuche in ILTUB-Transsonik-Windkanal." Fortschr.-Ber. VDI-Z., Reihe 7 Nr. 22, 1970